JOM, Vol. 64, No. 4, 2012
DOI: 10.1007/s11837-012-0302-8

The Structure, Functions, and Mechanical Properties of Keratin

J. McKITTRICK,[1,2,4] P.-Y. CHEN,[3] S. G. BODDE,[2] W. YANG,[2]
E. E. NOVITSKAYA,[2] and M. A. MEYERS[1,2]

1.—Department of Mechanical and Aerospace Engineering, UC San Diego, La Jolla, CA 92093, USA. 2.—Materials Science and Engineering Program, UC San Diego, La Jolla, CA, USA. 3.—Department of Materials Science and Engineering, National Tsing Hua University, Hsinchu, Taiwan, ROC. 4.—e-mail: jmckittrick@ucsd.edu

Keratin is one of the most important structural proteins in nature and is widely found in the integument in vertebrates. It is classified into two types: α-helices and β-pleated sheets. Keratinized materials can be considered as fiber-reinforced composites consisting of crystalline intermediate filaments embedded in an amorphous protein matrix. They have a wide variety of morphologies and properties depending on different functions. Here, we review selected keratin-based materials, such as skin, hair, wool, quill, horn, hoof, feather, and beak, focusing on the structure–mechanical property-function relationships and finally give some insights on bioinspired composite design based on keratinized materials.

INTRODUCTION

Keratin is a structural protein found in the integument (outer covering) in vertebrates; selected materials are listed in Table I. It is, after collagen, the most important biopolymer encountered in animals. Keratinized materials have a variety of morphologies that depend on the function. These range from a simple waterproof layer (turtle shell) to a structurally robust, impact-resistant material (horn). Keratin is both mechanically efficient in tension (wool) and compression (hooves). Similarities and differences are found with collagen, which is the other major structural protein in animals (bones, teeth, and connective tissue). Both have α-helix polypeptide chains that have a well-defined amino acid sequence. Both contain a high amount of the smaller amino acid residues, glycine and alanine, which makes the α-helical structure possible. In keratin, two polypeptide chains (α-keratin) twist together to form a coiled coil, whereas in collagen, three α-helices (tropocollagen) twist together and assemble to form the collagen fibril. One major distinction is that the keratinocytes (keratin-producing cells) die after producing keratin; thus, keratin is a "dead" tissue that is not vascularized, as opposed to collagen that forms in the extracellular matrix. For this reason, the most keratinized materials form polygonal tiles (tens of microns in diameter) that overlap laterally and are stacked on top of each other to form a relatively dense layer. Another distinction is that keratin can be considered as a composite material consisting of a short fiber (crystalline keratin)-reinforced polymer (amorphous keratin).[1] The crystalline component is insoluble in water, but the amorphous parts can absorb water and swell. Table II compares some mechanical properties of keratin and other biological fibrous materials. Keratin generally has a higher Young's modulus than collagen, yet it has tremendous strains to failure, indicating that keratin should have high toughness values.

Keratin has a large amount of cysteine residues, which have a thiol group (-SH), producing a strong, covalent disulfide bond that cross links the polypeptide chains together and also cross links the matrix molecules. This process is similar to what occurs during the vulcanization of rubber. Keratins can be classified as "hard" or "soft"–softer keratin has less sulfur and therefore fewer cross links. Soft keratin is almost exclusively as the outermost layer of the skin (epidermis).

Structure

The basic macromolecules that form keratin are polypeptide chains. These chains can either curl into helices (the α-conformation) or bond side-by-side into pleated sheets (the β-conformation). Mammals have approximately 30 α-keratin variants that are the primary constituents of hair, nails,

(Published online April 3, 2012)

Table I. Major keratin distribution in animals

	Order	Location
Mammal	Artiodactyla (cow, sheep, goat, and pig)	Hoof, horn, fur, wool, skin
	Perissodactyla (horse, tapir, and rhinoceros)	
	Cetacea (baleen whale)	Baleen
	Primate	Hair, nail, skin
	Monotremata (echidna)	Quill
	Insectivora (hedge hog, and tenrec)	Quill
	Rodentia (porcupine, spiny rat, spiny dormice, and cane rats)	Quill
	Xenarthra (armadillo)	Osteoderm covering
	Pholidota (pangolin)	Armor
Reptile	Testudina (turtle, tortoise, and terrapin)	Osteoderm covering
	Crocodilia (crocodile, alligator, and caiman)	Osteoderm covering
	Squamata (gecko)	Feet
Bird		Feather, beak, claw
Fish	Myxiniforme (hagfish)	Teeth, slime

Table II. Comparison of mechanical properties of keratinized structures and compared with other organic fibers

Source	RH (%)	Water Content (%)	E (GPa)	σ_f (MPa)	ε_f (%)	References
Collagen (along fibers)			1	50–100	0.09	2
Cellulose (flax)			100	840	0.02	2
Silk			10	600	0.2	2
Beak, toucan	50		1.5	30	0.1	3
Claw, ostrich	0		2.7	90	5.7	4
	50		2	69	6.7	4
	100		0.1	14	50.5	4
Hagfish slime threads		In water	0.006	180	220	5
Hair, human	70		1.5			6
				200		25
Hoof, bovine		30	0.4	16.2 14.3 (b)		7
Hoof, equine	41		0.2	19.4 (b)		8
	100		0.3–0.6	6.5–9.5		9
Horn, oryx		0	6.1	137		10
		20	4.3	122		10
		40	1.8	56		10
Horn, bighorn sheep		20	1.5			11
		10.6	2.2	127 (b)		12
		34.5	0.81	39 (b)		12
Nail, human	20		4.34			13
	55		2.34			13
	100		0.47			13
Quill, porcupine	65		1.9–2.3	63–170 (c)		15
	65		2.7	146	25	16
	100		1	60	49	16
Quill, hedgehog		Dry	3.8			17
		Wet	2.3			17
Stratum corneum	26		8.9		1.9	18
	68		2.4		7.7	18
	100		0.01		140	18
Wool, Cotswold	0		5.6			19
Wool, Lincoln	65		4.5			20
	100		2.5			20
		In water	3	150	45	5

All are tensile test results except (b) = bending and (c) = compression hooves, horns, quills, and the epidermal layer of the skin. In reptiles and birds, the claws, scales, feathers, and beaks are β-keratin, which is tougher than the α form, and it is configured into a β-pleated sheet arrangement. The setae of the gecko foot, which provide the strong attachment of the feet to surfaces, are also composed of β-keratin.

Figure 1a shows the molecular structure of α keratin.[21,22] Three distinct regions can be identified: the crystalline fibrils (helices), the terminal domains of the filaments, and the matrix. Isolated α-helix chains form a dimer (coiled coil) with sulfur cross links, which then assemble to form protofilaments. These protofilaments have nonhelical N- and C-termini that are rich in cysteine residues and cross link with the matrix. The protofilaments polymerize to form the basic structural unit, the intermediate filament (IF), with a diameter of ~7 nm and a spacing of ~10 nm apart. The IFs can be acidic (type I) or basic (type II). The IFs are embedded in an amorphous keratin matrix of two types of proteins, high sulfur, which has more cysteinyl residues, and high-glycine-tyrosine proteins that have high contents of glycyl residues.[20] The matrix has been modeled as an isotropic elastomer.[23] A transmission electron microscope (TEM) micrograph of ram horn keratin is shown in Fig. 1b—the dark strand is the crystalline IF, which is surrounded by the lighter amorphous matrix.[24]

The alignment of the IFs influences the mechanical properties. For example, the tensile strength of human hair (~200 MPa) is an order of magnitude greater than that of human nail[25] because of the higher order alignment of the keratin IFs in hair. The volume fractions of the matrix (amorphous) and crystalline fibers vary significantly in different materials. For example, the volume fractions of the matrix are 0.37, 0.42, and 0.54 for porcupine quills, wool, and human hair, respectively,[26] which roughly correlates with a decrease in Young's modulus.

The molecular structure of β keratin with a pleated structure is illustrated in Fig. 1c. The pleated sheets are composed of antiparallel chains.[27] Positioned side by side, two or more protein strands (β strand) link through hydrogen bonding. The linked β strands form small rigid planar surfaces that are

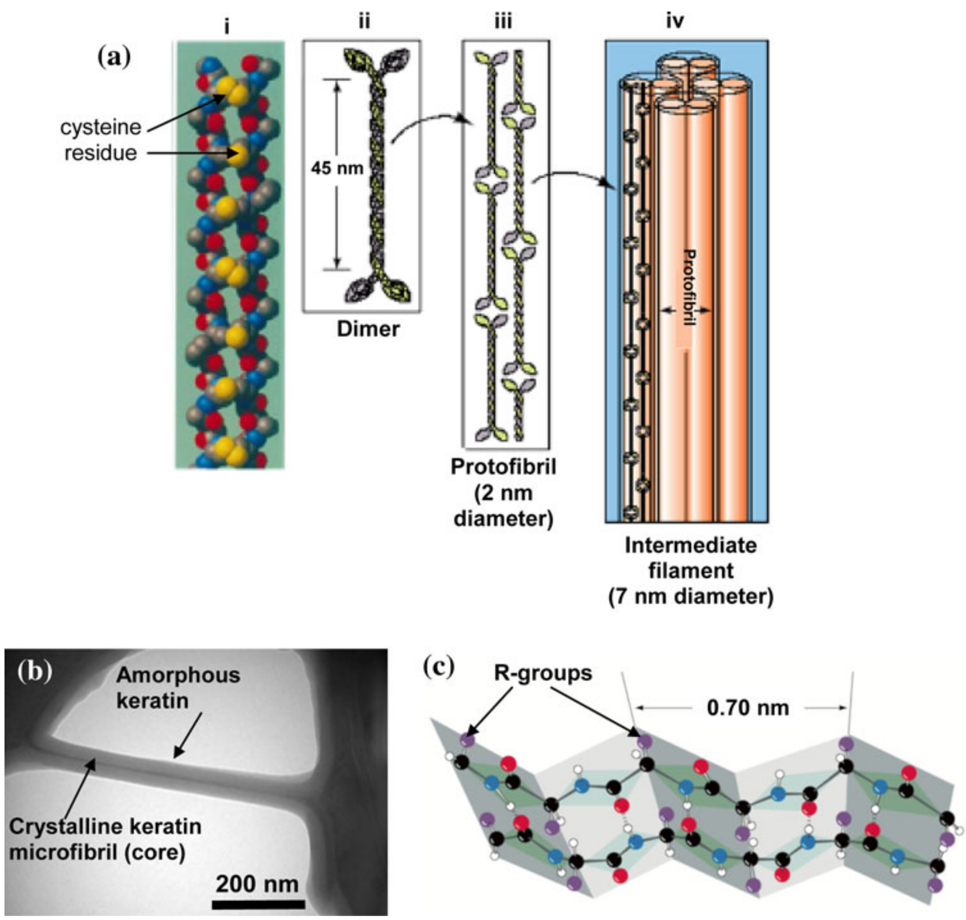

Fig. 1. (a) Molecular structure of α keratin: (left to right): (i) space-filling ball model.[21] (ii) Two keratin polypeptides form a dimeric coiled coil. (iii) Protofilaments form from two staggered rows of tail-to-head associated coiled coils. (iv) Protofilaments bimerize to form a protofibril, eight of which form an intermediate filament.[22] (b) TEM micrograph of α-keratin intermediate filament from a sheep horn. The strongly diffracting core of crystalline keratin is surrounded by an amorphous matrix.[24] (c) β-Pleated sheet configuration. Hydrogen bonding holds the protein chains together. R groups extend to opposite sides of the sheet are in register on adjacent chains (Figure © Irving Geis).

slightly bent with respect to each other, forming a pleated sheet arrangement. If the α-form is stretched, then it will transform to the β-form,[27] which is reversible up to approximately 30% strain.

In this article, we provide a broad and introductory presentation of the structure and mechanical properties of various keratinous materials. It is divided into functional sections: protection and covering, defense and aggression, motion, and finally some thoughts on bioinspired materials and structures based on keratinized materials. We mainly focus on the work performed in our laboratory.

PROTECTION/COVERING

Skin: Stratum Corneum

The outermost layer of the skin is the epidermis, which varies from 30 μm (eyelids) to 1 mm (soles of feet) thickness in humans (Fig. 2a), and serves as a barrier to protect the underlying tissue from infection, dehydration, and chemical and mechanical stresses. Keratinocytes make up more than 95% of the epidermis cells. The stratum corneum (10–20 μm) is the outermost layer (soft keratin) and is constantly shed (Fig. 2b). It consists of overlapping scales (Fig. 2c), a morphology that is characteristic of almost all keratinized materials.

Mechanical tests on the stratum corneum show the Young's modulus to range from 0.01 GPa to 9 GPa, which is highly dependent on the relative humidity and temperature.[18,28] Failure strains up to 140% were found in 100% RH at room temperature for rat skin.[18] Soft keratin is formed by loosely packed bundles of IFs embedded in the amorphous matrix,[29] in contrast to hard keratin, which is formed by ordered arrays of IFs embedded in an amorphous α-keratin matrix.

Wool and Hair

The early work on keratinized materials, motivated by the textile industry, has been on wool. Hair, wool, and fur are shafts of circumferential layers of dead cells that have grown from follicles in the skin. Figure 3a shows the hierarchical structure. The outermost layer (cuticle, ~10%) consists of overlapping cells that adhere to the root shaft to anchor the hair firmly in the follicle. The middle layer (cortex, ~90%) has keratinized cells and pigment. In fine hair, the medulla (hollow core) is not present. During the growth phase, some epidermal cells keratinize and die, and then are pushed outward forming the cortex and outer cuticle. Wool fibers are slightly elliptical, with mean diameters between 15 μm and 50 μm and have an average density of 1.3 g/cm^3. They decompose ~130°C and grow at a rate of ~10 cm/year. At 65% relative humidity (RH), wool can absorb 14–18% water. The keratin fibers are embedded in cells held together by the lipid-rich cell membrane complex. On the surface, there are several layers in the cuticle, which have overlapping scales. Because keratin filaments are produced in cells, which then die after the keratinization process is complete, remnants of the cell walls remain. Figure 3b–e shows some interesting cross sections of hair from a rabbit, an elk, a polar bear, and a human. It has been reported widely that the excellent thermal insulation of polar bear hair is because of the hollow core; however, it is observed that other species also have a hollow core, including human hair.

Figure 4a is a typical tensile stress–strain curve for hydrated wool. An initial uncrimping region exists that is followed by a linear elastic region up to the yield point, at ~2% strain. At the yield stress, the α- to β-keratin transformation is initiated in the

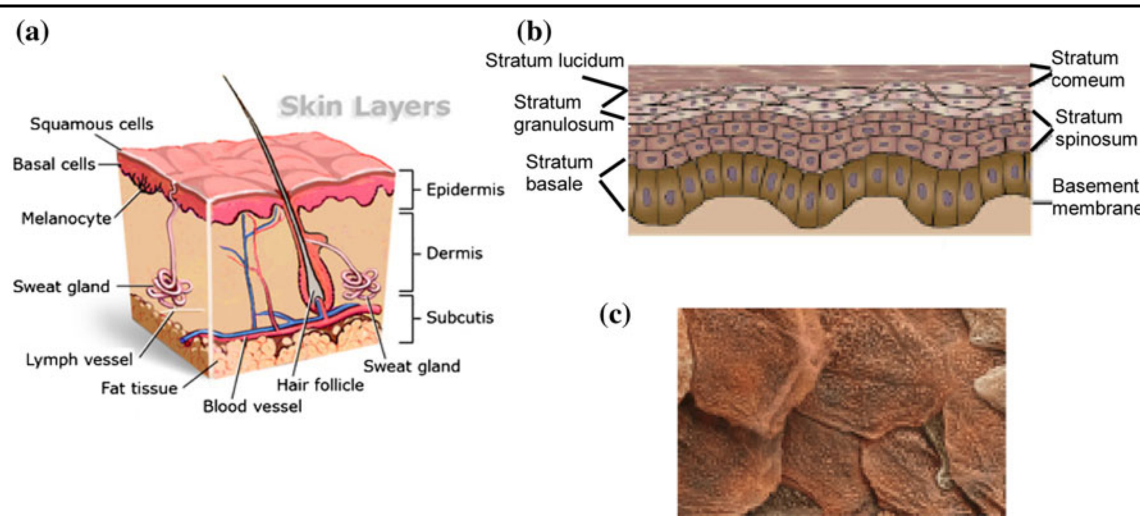

Fig. 2. Layers in the skin. (a) Skin has three main layers, from top to bottom—the epidermis, dermis, and subcutaneous fat. (b) The epidermis (95% keratinocytes) consists of five layers, which migrate continually from the stratum basale to the stratum corneum. Keratinization begins in the stratum spinosum. (c) SEM micrograph of the overlapping scales of the stratum corneum (Photograph by Andrew Syred/Science Photo Library, National Geographic, http://heartspring.net/skin_cancer_symptoms_treatments.html).

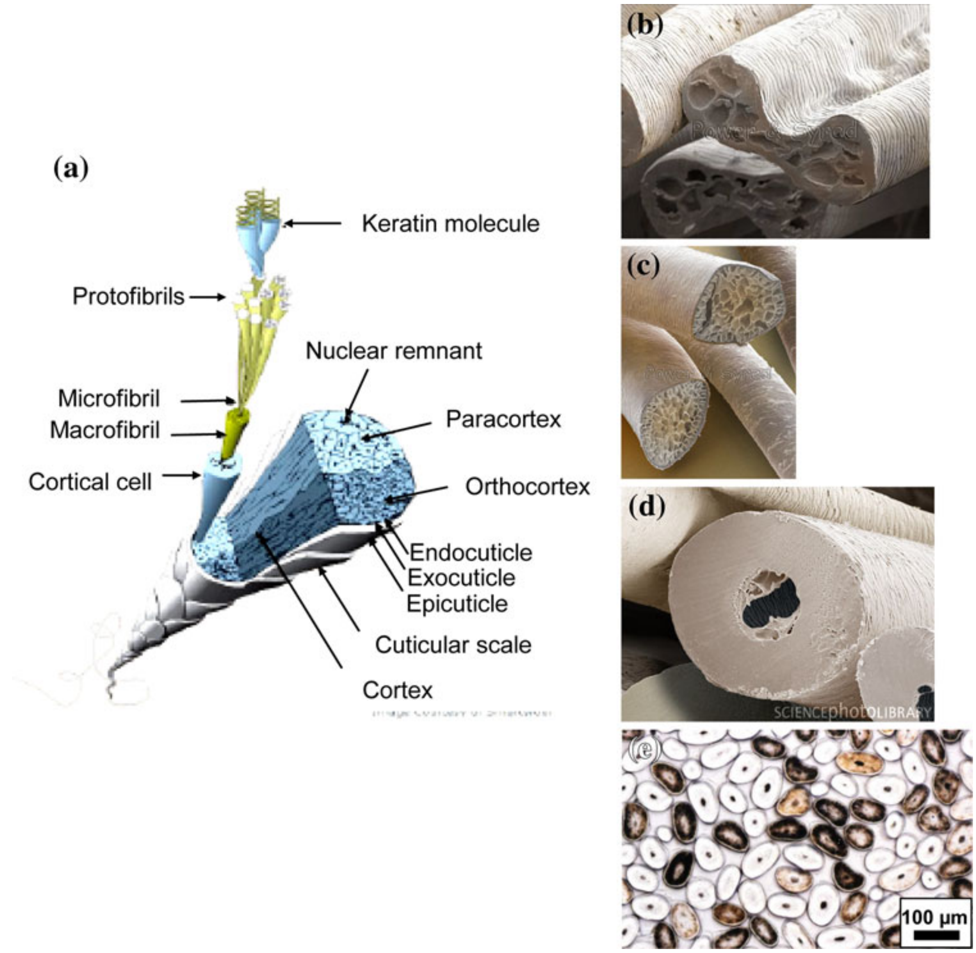

Fig. 3. (a) Hierarchical structure of wool fibers. The scaly exterior layer of a wool fiber is called the cuticle and is overlaid with the epicuticle that is coated with lanolin, which is a waxy, water-shedding film. The epicuticle and its waxy coating is what confers wool's resistance to mist and light rain http://www.rei.com/expertadvice/articles/wool+clothing.html. Cross-sectional SEM images of the morphologies of hair and fur: (b) common European rabbit (*Oryctolagus cuniculus*), (c) elk (*Cervus elaphus*), and (d) polar bear (*Ursus maritimus*). All photos are from http://www.psmicrographs.co.uk. (e) Human hairs from a 60-year-old female. http://www.pgbeautygroomingscience.com/breakthroughs-xxiii.html.

IFs. At ~30% strain, the slope increases abruptly. This has been attributed to either strain hardening of the elastomeric matrix[23,30] or to the opening of remaining α-helices.[31] Continued loading produces some cross-link rupture in the IFs, and fracture occurs between 50% and 60% strain. One interesting feature of wool and hair is that complete recovery (up to the end of the yield region) can be achieved if the fibers are subsequently soaked in warm water after testing. Figure 4b illustrates Fueglelman's[32] concept of the nanoscopic deformations of the constituents. In Fig. 4b(i), the unstretched components are shown—the IFs rods, the amorphous matrix, and water-containing globules in the matrix. Deformation pushes the IFs together and squeezes the matrix, as shown in Fig. 4b(ii). Two zones, X and Y, account for the yield and post-yield behavior (Fig. 4b(iii)). The stress–strain response is analogous to that of the well-known shape-memory alloys. In the latter, the total strain only reaches 6%, whereas in wool it is much larger.

The profound influence of hydration on the mechanical properties is illustrated in Fig. 4c, which shows stress–strain curves for wool tested in water at different temperatures (Fig. 4c(i)) or tested at different RH (Fig. 4c(ii)).[33] At lower temperatures, the stress–strain curves have a similar shape to that in Fig. 4a, although the yield and fracture stresses decrease accompanied with a decrease of the linear elastic and increase of the yield regions. At higher temperature, the abrupt increase in slope after the yield region is absent. A similar trend is observed with an increase in RH. One interesting feature is that the Young's modulus seems to be constant for all test conditions.

Quills and Spines

Porcupines, hedgehogs, echidnas, tenrecs, and spiny rats are covered by quills that protect the animal from aggressors. In all, 29 species of porcupines are distributed throughout most areas in the

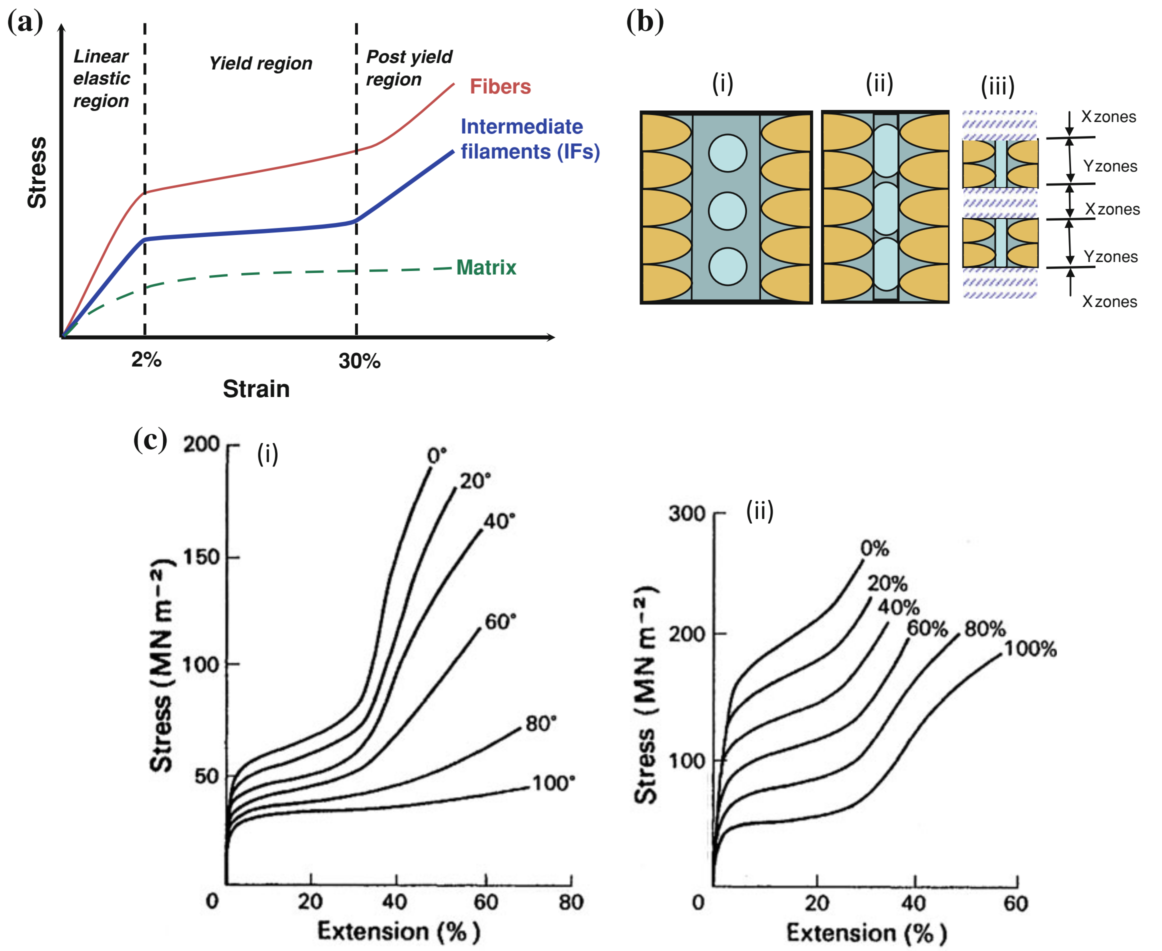

Fig. 4. (a) Schematic representation of a stress–strain curve for a wool fiber, showing the contributions of the intermediate filaments and matrix.[31] (b) Feughelman's model showing zones, X and Y. The X zones contribute to the deformation of the yield region and the Y zones contribute to the deformation of the postyield region. (i) Matrix consists of water-containing globules. (ii) As the load is applied, the IFs move toward each other, jamming the protein residuals. (iii) With protein residuals jammed by two intermediate filaments, the Y zones become more difficult to extend.[32] (c) Stress–extension curves for wool: (i) in water at various temperatures and (ii) at different relative humidities[33]

world. They are divided into two main families: Old World (Hystricidae) and New World (Erethizontidae). Both families have muscles at the base of the quill allowing them to stand up, thereby making the animal look larger if threatened. The Erethizontidae quills can be as long as 8 cm, whereas the Hystricidae are longer—up to 50 cm—and also have a proportionally larger diameters.[17] Porcupine quills are the hard form of keratin with a modulus around 5.6–6.0 GPa.[17,20] As with other keratinous materials, the mechanical properties are highly dependent on the amount of hydration, relative humidity, and temperature.

Quills with their analog in the flora world, plant stems, are designed to resist axial loads and bending moments that produce Euler buckling.[17,34]

All porcupine quills consist of a stiff outer sheath (cortex) and a compliant, porous foam (core), an assembly that is similar to the feather rachis. This configuration maximum the flexure strength/weight ratio. The keratin filaments align along the long axis of the quill resulting in different mechanical properties in the transverse and longitudinal directions.[20] Quills can take on four microstructural arrangements, as follows[17,34]:

1. Dense outer sheath with an interior foam (New World porcupines, echidnas)
2. Same as (1) but with longitudinal "stiffeners" that show a spoke-like pattern in the cross-sectional image (Old World porcupines)
3. Same as (2) but with transverse stiffners (septae) (hedgehogs)
4. The foam consists of closely spaced septae (tenrec)

Figure 5 shows scanning electron microscope (SEM) images of the structure of the Erethizontidae (*Erethizon dorsatum*) and Hystricidae (*Hystrix*) quills in the longitudinal and transverse directions.[15] The foam cells (Fig. 5a, d) increase in size gradually from the edge of the cortex to the center. The foam is isotropic, as observed in the longitudinal images in Fig. 5b and e. The surfaces consist of overlapping keratin scales (Fig. 5c, f). On the

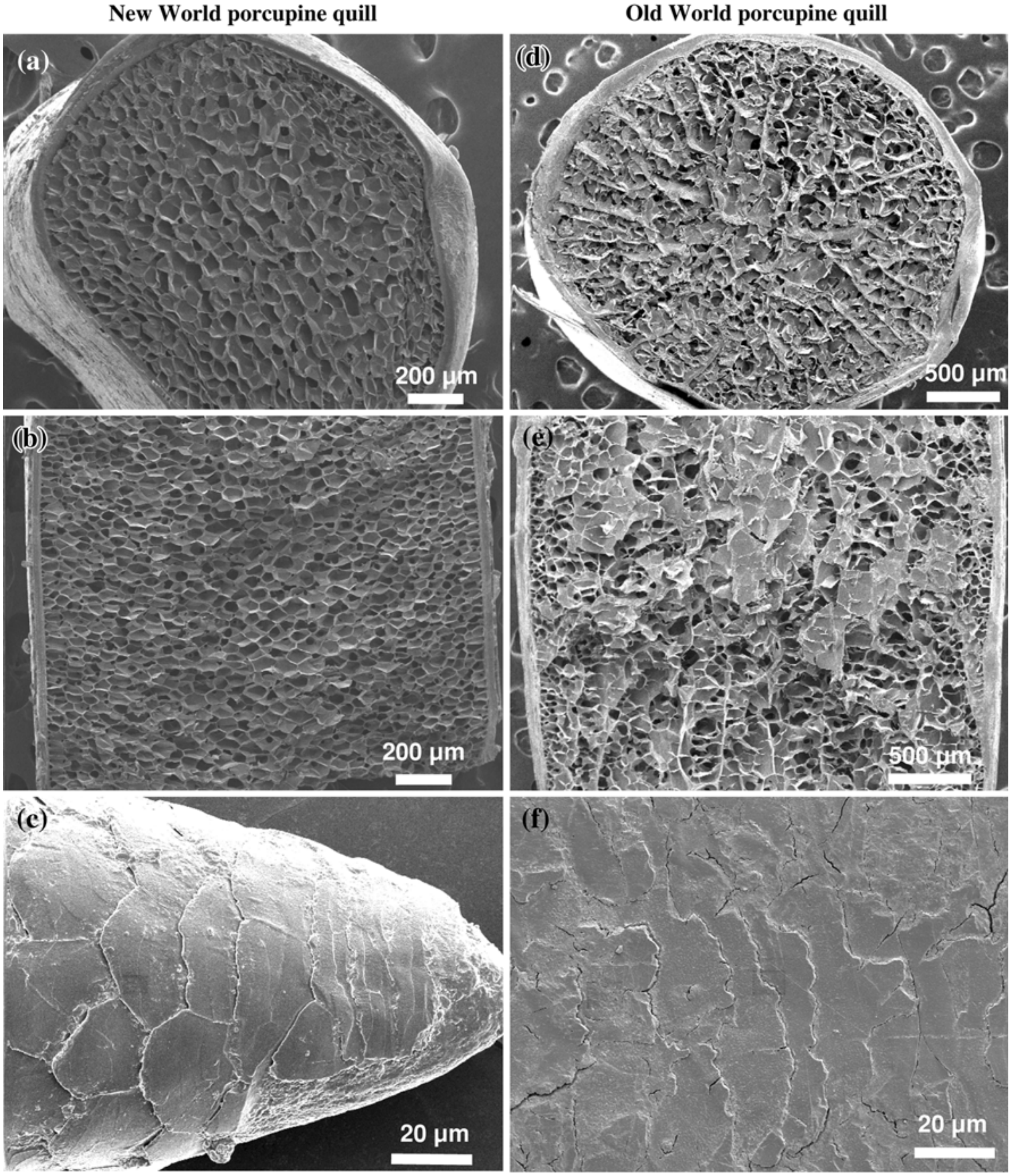

Fig. 5. SEM images of (a, d) transverse, (b, e) longitudinal cross-sections, and (c, f) tip surfaces of New World (Erethizontizae) and Old World (Hystricidae) quills, respectively.

Erethizontidae quills, the keratin scales are arranged to provide a smooth insertion surface and a rough surface as it is pulled out (i.e., a barb). An impaled quill would cause pain to predators when they try to remove the quill.

The important properties of the foam are the bulk and relative densities. The density of the foam (ρ_f) divided by the density of a completely dense solid composed of the cell wall material (ρ_w) defines its relative density (ρ_f/ρ_w). Based on the core to cortex density ratio, the ratio of Young's modulus of a cellular solid to that of the solid cell wall materials can be estimated. Using Gibson and Ashby's models[35] for cellular solids, a relative Young's modulus of the close cell foam core in Erethizontidae can be estimated as

$$\left(\frac{E_f}{E_w}\right) = \left(\frac{\rho_f}{\rho_w}\right)^2$$

where E_f and E_w are Young's moduli of the cellular solid and solid cell wall material, respectively. For

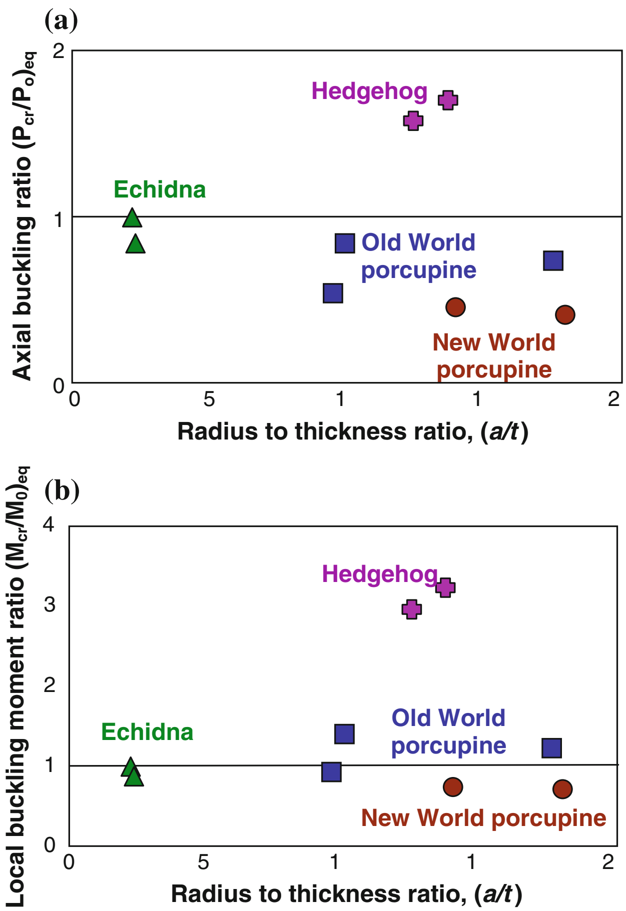

Fig. 6. Ratio of the failure loads of quills and spines to those of a cylinder with no porous core (equal radius and mass): (a) axial buckling and (b) local buckling[34]

porcupine quills, $\rho_f/\rho_w \sim 0.1$, yielding a relative Young's modulus of ~0.01.

Vincent and Owers[17] examined the Euler buckling conditions for quills for a variety of species. The denser cortex provides resistance to buckling, whereas the foam acts as an elastic foundation that provides local support to the cortex and significantly delays the onset of local buckling.[36,37] The hedgehog spines are found to be designed to resist impact (either through falling or from a predator), whereas the porcupine spines are designed to pierce opponents. The proximal ends of the hedgehog spines are mushroom shaped so that they do not pierce the host animal during a fall.

In comparison with intact quills, the cortex performs the same in compression (axial loading) but behaves poorly in bending tests. Karam and Gibson[34] estimated the contribution of the foam to local elastic buckling resistance. Figure 6 shows plots of the axial and local buckling moments of quills and spines compared with equivalent hollow cylinders. The hedgehog spines stand out as having the maximum resistance to buckling, and it was concluded to be the optimal design for lightweight, biomimetic columns that resist buckling. Indeed, hollow structures filled with foam have considerable potential for lightweight structural applications, and are being introduced into the automotive industry.[38]

Figure 7a shows typical compression stress–strain curves for short (non-Euler) specimens of Erethizontidae (*E. dorsatum*) and Hystricidae (*Hystrix*) whole quills and quills with the foam removed (cortex only).[15] The intact quills for both species show a higher Young's modulus, compressive strength (onset of local buckling), and toughness than that of the cortex alone, which indicates that the foam influences the local buckling behavior significantly. Figure 7b shows the compression stress–strain curve for the *Hystrix* foam, illustrating that it behaves as a classic polymeric cellular solid—a linear elastic region followed by a plateau region where the cell walls bend and deform, followed by an upturn in the curve where all the cell walls have collapsed and the material densifies. Figure 7c through f shows the damage incurred from an interrupted test of an *Erethizon* quill (before complete densification). Local plastic buckling of the cortex (Fig. 7c, d) is accompanied by a high degree of both tensile and compressive deformation of the foam (Fig. 7d, e). Compressive deformation occurs around the buckled cortex regions; however, most of the foam is in transverse tension in the central region (dashed rectangle). The tensile stress causes small tears in the foam walls (arrow in Fig. 7f). It is clear that the foam remains attached firmly to the cortex, providing enough support to delay local plastic buckling of the cortex (Fig. 7d, e).

In tension, the interior foam was also found to have a negligible effect on the Young's modulus of Hystricidae and Erethizontidae quills, and they observed that the cortex has 2–3 concentric layers, which is similar to what is found in the feather rachis.[16]

Pangolin Armor

An unusual armor is found on the pangolin. The pangolin is a small insectivore that lives in the rain forests of Asia and Africa. It ranges from 40 cm to 100 cm in length and weighs up to 18 kg. The exterior of the animal is covered with keratin scales, as shown in Fig. 8a, which weight up to 20% of the total animal. When curled up, these scales extend from the body, producing a barrier of razor-sharp edges (Fig. 8b). These scales have been used to create a coat of armor that was presented to King George III (Fig. 8c).

DEFENSE/AGGRESSION

Horns

Horns appear on animals from the Bovidae family, which includes cattle, sheep, and goats; they are tough, resilient, and highly impact resistant. In the

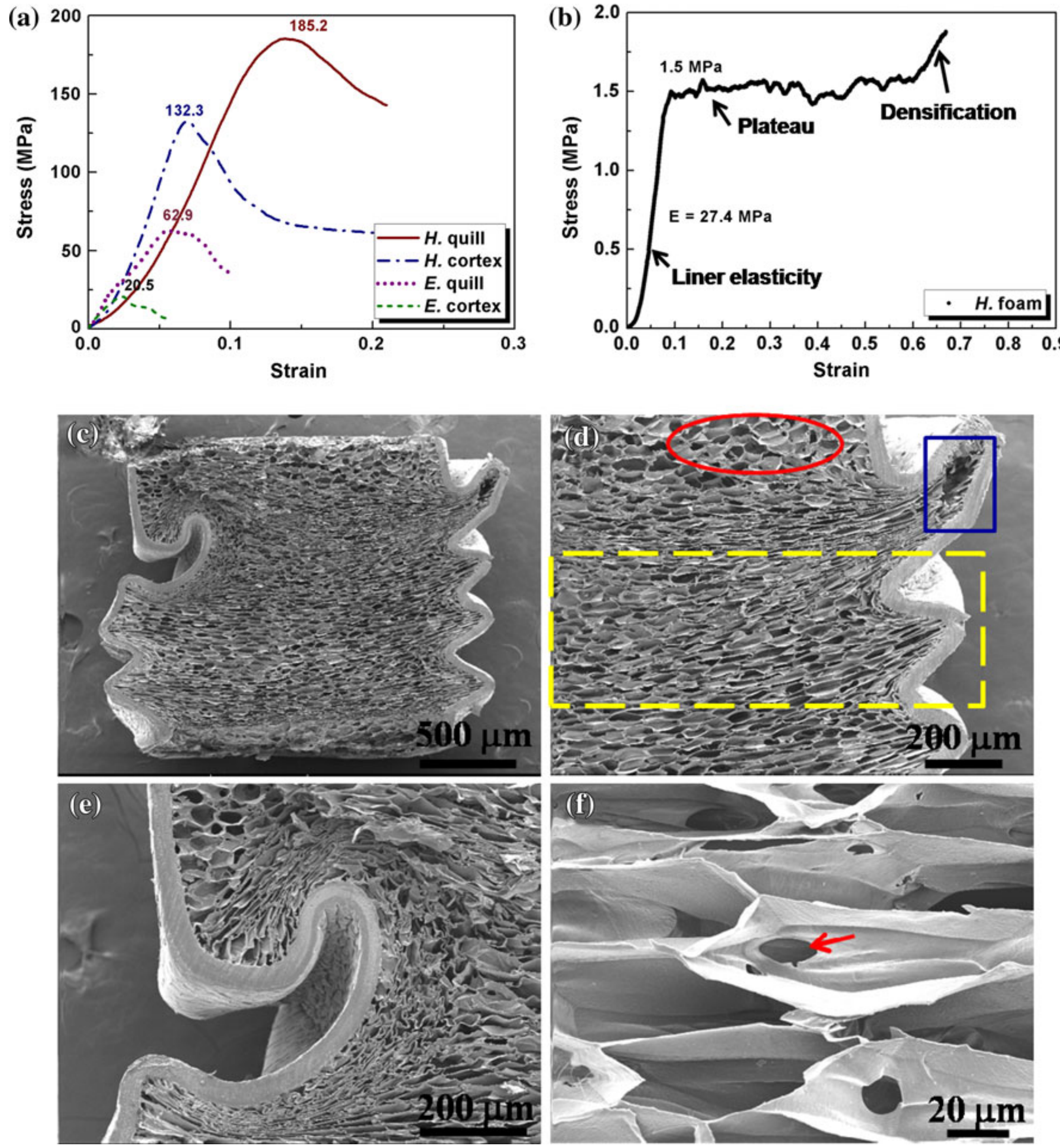

Fig. 7. Representative compression stress–strain plots of (a) whole quill (cortex and core) and cortex (core scraped out) of New World (Erethizontizae) and Old World (Hystricidae) porcupines and (b) foam of Old World porcupine. (c–f) SEM micrographs of a compressed *Erethizon* quill: (c) morphology of cross section, (d, e) foam and cortex at the buckling part, and (f) damaged cores. The dashed rectangle indicates tensile deformation. The arrow in (f) points to a tear produced by compressive load[15]

case of male bighorn sheep, the horns must be strong and tough as they are subjected to extreme loading impacts during the life of the animal and, unlike antlers, will not grow back if broken. On the living animal, horns encase a short bony core (*os cornu*) composed of cancellous bone covered with skin, which projects from the back of the skull. There is a variety of horn shapes and sizes, from the stumpy horns on domestic cattle to the extravagant forms observed on the greater kudu (helicoidal) (*Tragelaphus strepsiceros*), blackbuck (*Antilope cervicapra*), and the Nubian ibex (*Capra nubiana*).

Figure 9a shows the hierarchical structure of horn from a desert bighorn sheep (*Ovis canadensis*). The structure consists of keratin lamellae periodically separated by tubules that extend the length of the horn. The resulting structure is a three-dimensional, laminated composite that consists of fibrous keratin; it has a porosity gradient across the thickness of the horn. A cross-sectional optical micrograph (Fig. 9b) shows a lamellar structure with elliptically shaped porosity interspersed between the lamellae. The lamellae are 2–5 μm thick with the pore sizes ranging from 60 μm to 200 μm along the long axis of the pores.

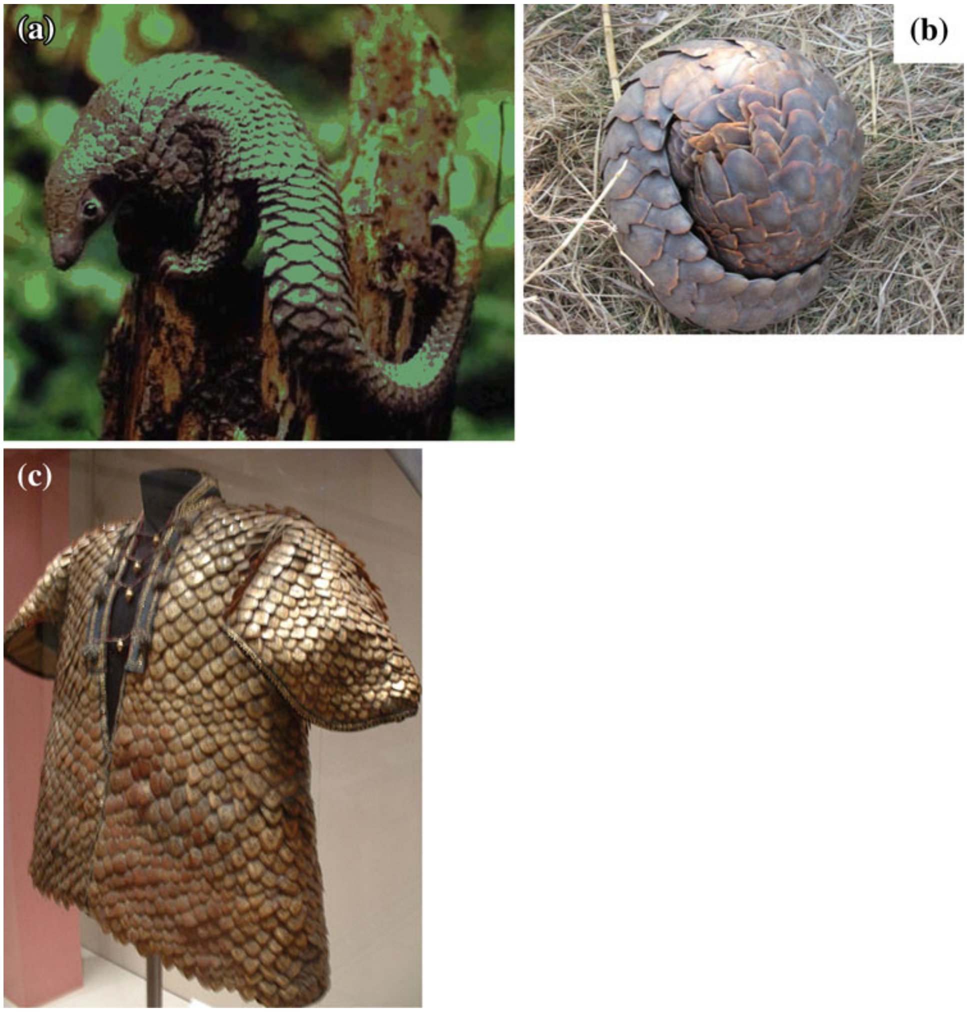

Fig. 8. (a) Pangolin (*Manis temmincki*) showing scaly exterior made of keratin. (b) The animal can curl into a ball to protect its interior organs (http://letopis.kulichki.net/2001/image2001/pangolin.jpg). (c) Pangolin armor presented to King George III in 1820.

Kitchener[10,39,41–43] and Kitchener and Vincent[40] were the first to provide insights into the fighting behavior of various species in the Bovidae family. Mechanical property measurements (strength, stiffness, and work of fracture—see Table II) revealed that horns are capable of high energy absorption before breaking and that hydration is important for decreasing the notch sensitivity. The critical crack length for crack propagation was calculated to be ~60% of the transverse dimension of the horn, indicating the superior flaw sensitivity of the material. The work of fracture (10–80 kJ/m^2) was found to be greater than most other biological and synthetic materials (antler: 6.6 kJ/m^2; bone: 1.6 kJ/m^2; glass: 5 J/m^2; mild steel: >26 kJ/m^2).[10] The fracture resistance was attributed to crack arrest and deflection mechanisms such as delamination and keratin fiber pullout. Kitchener and Vincent[40] examined the effect of hydration on the elastic modulus of horns from the oryx (*Oryx gazella*). They considered the structure of the horn as a chopped fiber composite, where the crystalline α-keratin fibers (40 nm long) were embedded in an amorphous keratinous matrix. Applying the Voigt model and using a chopped fiber composite analysis with a volume fraction of fibers as 0.61, they predicted a value of the elastic modulus close to the experimental value, indicating that a fibrous composite model of horn keratin is a reasonable assumption. As with other keratin-based materials, the elastic and shear modulus decreased significantly with an increase in the moisture content.[10,40]

Tombolato et al.[12] studied microstructure, elastic properties, and deformation mechanisms of desert bighorn sheep. Compression and bending tests were performed in both hydrated and ambient dried conditions. The elastic modulus and yield strength were found to be anisotropic and correlated with the orientation of tubules. Three-point bending tests showed that the elastic modulus and strength are higher in the longitudinal orientation (tubules parallel to the growth direction of the horn) than those in the transverse orientation (tubules perpendicular to growth direction of the horn). Trim et al.[44]

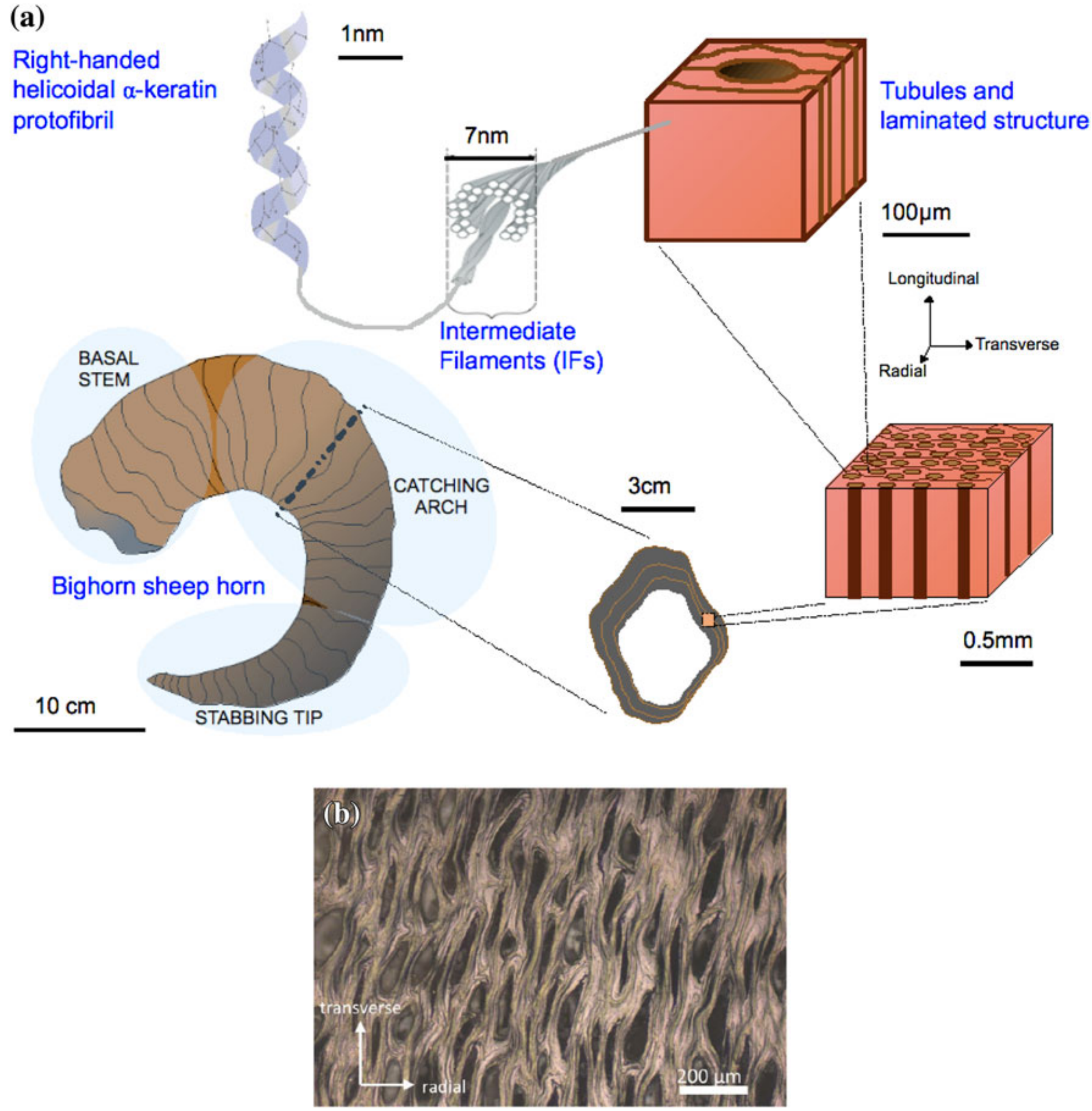

Fig. 9. (a) Hierarchical structure of bighorn sheep horn. The horns show a spiral fashion with ridges on the surface, which correspond to the seasonal growth spurts. The horns are composed of elliptical tubules embedded in a dense laminar structure. Each lamina has oriented keratin intermediate filaments interspersed in a protein-based matrix. (b) Cross-sectional optical micrographs of the horn showing the elliptical-shaped tubules[12]

investigated the mechanical behavior of bighorn sheep horn under tension and compression in hydrated and dry conditions. They found that tensile failure occurred by matrix separation followed by fiber pull out. The horn keratin failed in a brittle manner in the dry condition, whereas wet horn keratin was much more ductile. Compressive failure occurred by microbuckling followed by delamination, in agreement with Tombolato et al.[12]

Lee et al.[45] investigated the dynamic mechanical behavior of a wide range of biological materials (abalone nacre, elk antler, armadillo carapace, bovine femur, steer horns, and ram horns) and compared them with synthetic composites using a drop weight impact-testing systems. The impact strengths of horns were found to be the highest among biological materials, confirming the exceptional energy-absorbing capability of horn.

Claws and Nails

Claws and nails have not yet been studied in detail. Bonser and coworkers[4,46,47] measured the Young's modulus of ostrich claws (Table II). The difference between the longitudinal (along length of claw, Young's modulus ~1.8 GPa) and transverse (Young's modulus ~1.33 GPa) was 28%, which is a much larger anisotropy than what is reported for other keratinized materials such as porcupine quills (10%) and horsehair (5%), but is similar to the horse

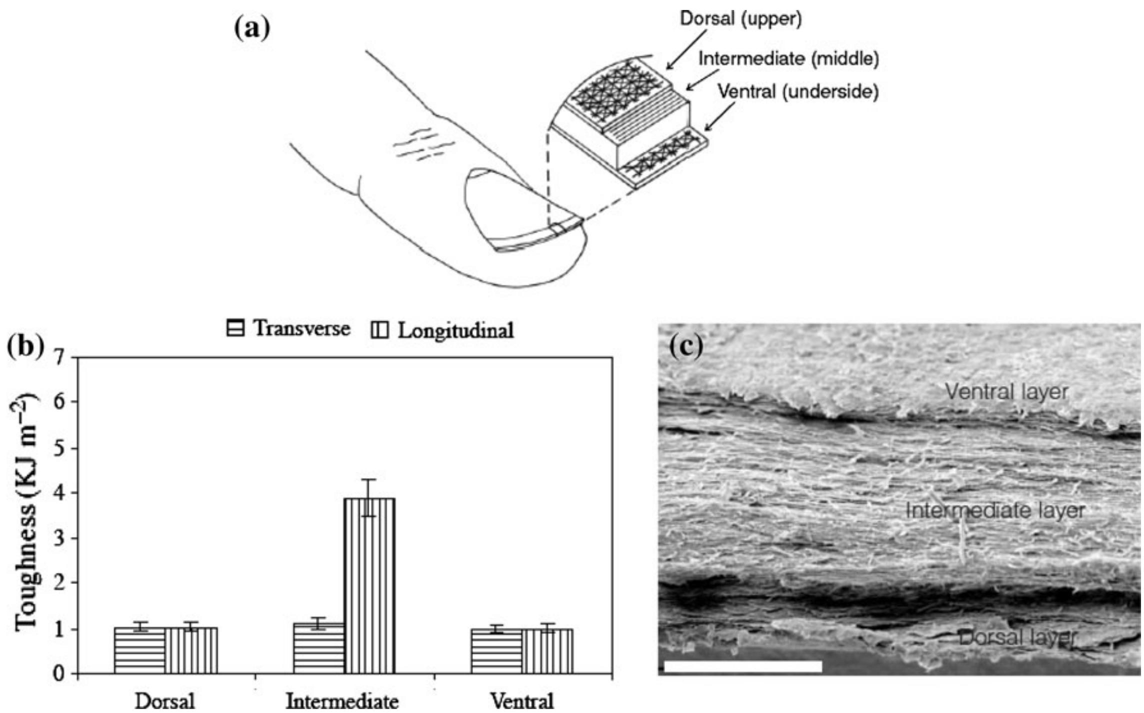

Fig. 10. Structure of the human nail: (a) Relative thicknesses of the layers of the nail, (b) toughness in the transverse and longitudinal direction for the three layers, and (c) SEM image of the cross section of a fracture surface (scale bar = 200 μm)[48,49]

hoof (10–40%). This anisotropy in claws and hooves was speculated to be caused by the multiaxial loading conditions to which they are subjected during movement, where a highly anisotropic material could fail under off-axis loading.[46]

Fingernails prevent the skin from the fingertips from rolling back and assist in gripping and manipulating objects. Mechanically, they can used to lift or pry open objects and for scratching and fighting. The nails are designed to resist bending forces, which is accomplished by the shape and also the orientation of the keratin filaments. It was reported (x-ray diffraction) that the keratin fibers are oriented transversely across the nail.[6]

Primate nails are sandwich structures consisting of three layers: a thin dorsal layer that is a moderately hard keratin, a thick middle layer that is harder and thicker, and finally a soft ventral layer. The middle layer has well-aligned keratin fibers oriented in the transverse direction, whereas the dorsal and ventral layers show no preferred orientation (Fig. 10a).[48,49] The toughness values are highest for the middle layer tested in the longitudinal direction, demonstrating that the preferential alignment of the keratin fibrils serves to stop cracks running down the length of the nail (Fig. 10b). This high ratio is similar to what is found in horse hooves.[9] It seems that the purpose of the ventral and dorsal layers is to provide mechanical support if the nail is loaded unevenly. A transverse fracture surface is shown in Fig. 10c. The dorsal surface has flat, overlapping scales in the plane of the nail. The intermediate layer is more fibrous, and clear fiber orientation is observed with a corresponding smooth fracture surface. The fracture surfaces of both dorsal and ventral layers are more jagged, indicating that the keratin fibrils are oriented randomly.

Beaks

Bird beaks serve a variety of purposes: eating and probing for food, fighting, courtship, grooming, killing prey, and exchanging heat. A wide variety is found in the morphology, color, and size but all have mandibles (bone) that project from the head that are covered by a β-keratin layer. Birds usually have either short or thick beaks or long and thin beaks. Exceptions are toucans and hornbillls, which have both long and thick beaks. The Toco Toucan (*Ramphastos toco*) has the largest beak among the species. The toucan beak is one-third of total length of the bird; nevertheless, the weight is 1/30th to 1/40th of its mass. The outside shell of beak consists of β keratin. The inside is filled with a cellular bone. This internal foam has a closed-cell structure constructed from bony struts with thin membranes.

Figure 11a through c shows photographs and schematics of the toucan beak.[50,51] The keratin shell consists of polygonal tiles 30–60 μm in diameter and 2–10 μm thick (Fig. 11d). TEM images of the longitudinal and transverse sections are shown in Fig. 11e. The keratin tile boundaries are wavy and traced by black lines for greater clarity. They are shown in the longitudinally sectioned beak keratin. The IFs are distributed in the amorphous keratin matrix, indicated by arrows. There seems to be a

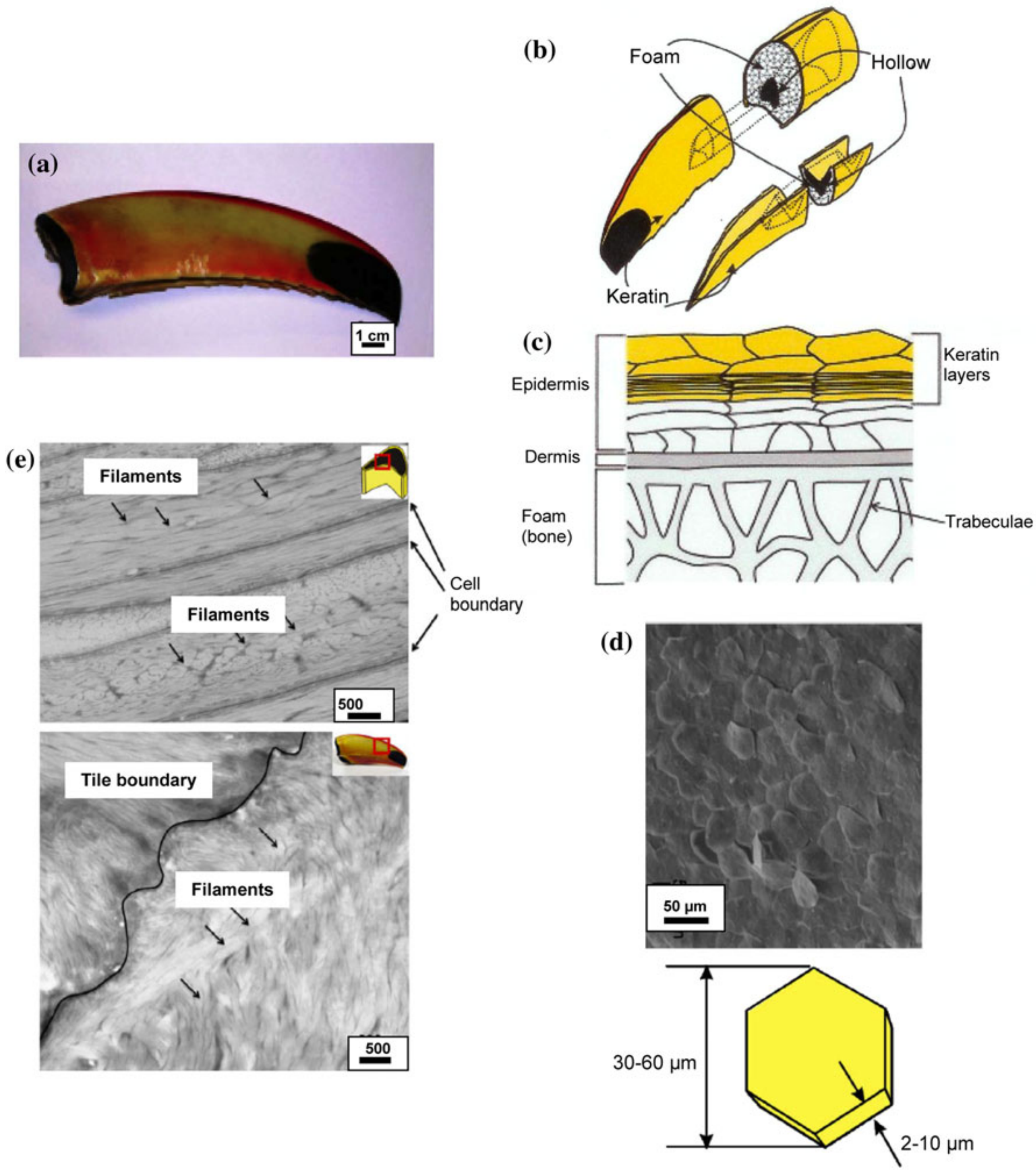

Fig. 11. (a) Photograph of a Toco Toucan beak, (b) overview diagram of the keratin and foam in the beak, (c) schematic illustration of a cross section from the outer region. The keratin layer is 500 μm thick, (d) SEM image of the keratin tiles on the surface of the beak, (e) TEM micrograph of the transverse cross section (top) and longitudinal surface (bottom) showing the keratin intermediate filaments.[50,51]

difference in orientation of the IF from layer to layer, similar to a 0°/90° laminated composite. The elastic stiffness of the beak keratin was found to be isotropic in the transverse and longitudinal directions.[3] The surface tiles exhibit a layered structure, and the tiles are connected by organic glue. The intermediate filaments, embedded fibers in the keratin matrix, seem to be aligned along the cell boundaries. These tiles undergo a peculiar behavior known in metallurgy as a ductile-to-brittle transition. As the strain rate is increased, the yield strength increases significantly. In this region, the fracture transitions from intertile (tile pullout) to transtile (tile fracture) because of the existence of two competing failure processes with different strain-rate sensitivities.

Seki and Meyers[3] found the toucan beak to have a bending strength (Brazier moment) that is considerably higher than if all the mass were concentrated in the shell as a solid hollow cylinder by applying the analysis developed by Karam and Gibson.[52] Seki and coworkers[3,50] showed that the internal cellular core

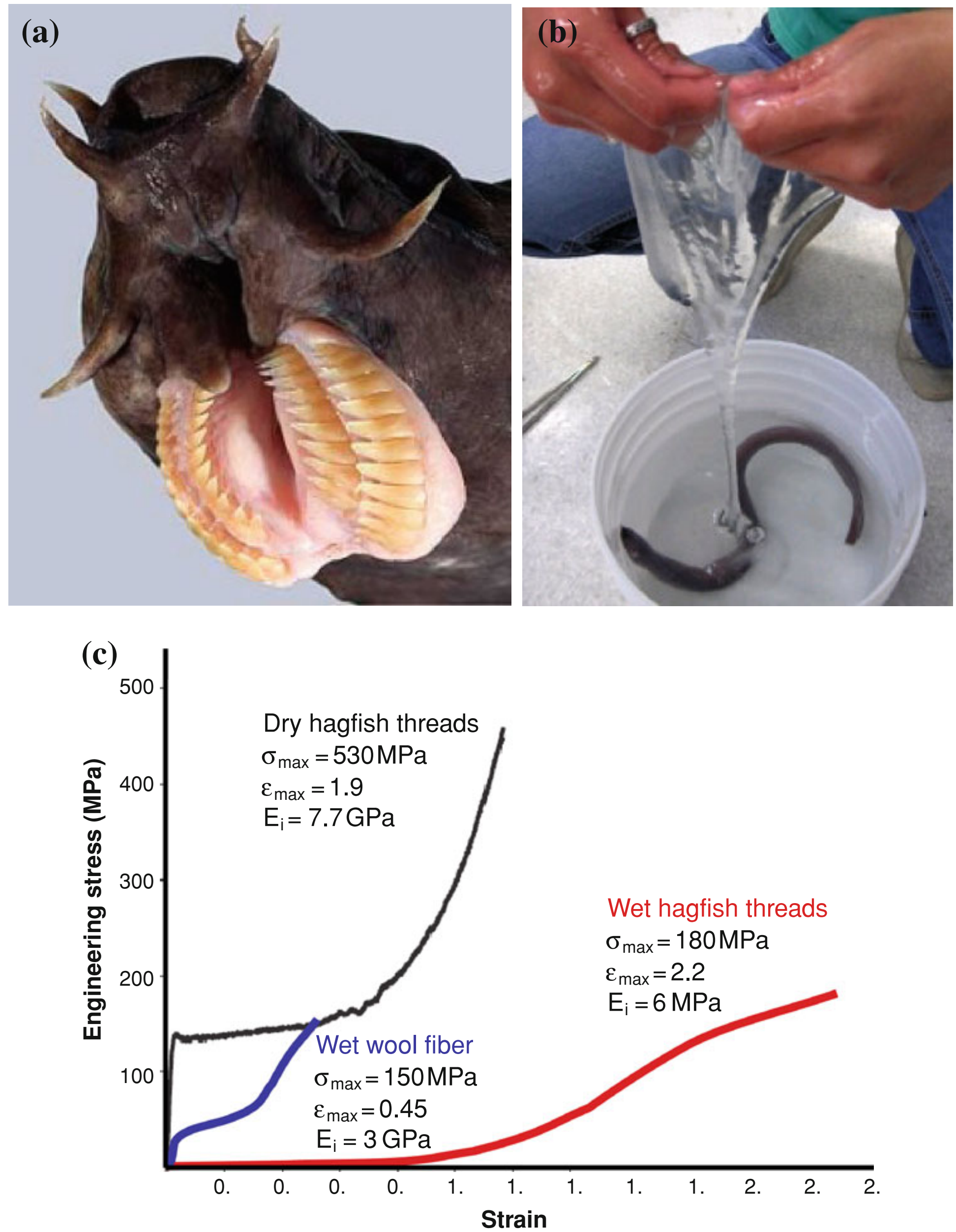

Fig. 12. (a) Photograph of a Broadgilled hagfish (*Eptatretus cirrhatus*) tongue with keratin teeth. Photography by Carl Struthers © Museum of New Zealand Te Papa Tongarewa. (b) Slime produced by one hagfish (http://www.people.fas.harvard.edu/~lim/research.htm). Stress–strain curves for (c) wet wool fibers and wet and dry hagfish threads[57]

serves to increase the buckling resistance of the beak and demonstrated a synergism between the two components that provides the stability in bending configuration. Thus, there is clearly an advantage in having internal foam to support the shell. The same conclusion is reached with quill and feather studies regarding the role of the internal foam.

The mechanical behavior of the bird beaks is governed by both the ductile keratin integument and semibrittle bony foam. Most of the mechanical loading on the beak is carried by the exterior keratin, whereas the foam increases the energy absorption and stabilizes the deformation of the beak to prevent catastrophic failure.[3] In the case of the toucan, the beak is mainly for the apprehension of food so that it is designed to resist bending moments. Indeed, the beak design is such that the hollow core provides an additional weight gain, since the bending stresses are directionally proportional to the distance from the neutral axis.[3]

Teeth

The most ancient vertebrates are in a class of fish, Agnatha (lampreys and hagfish), which do not have jaws but sharp conical teeth composed of keratin.[53]

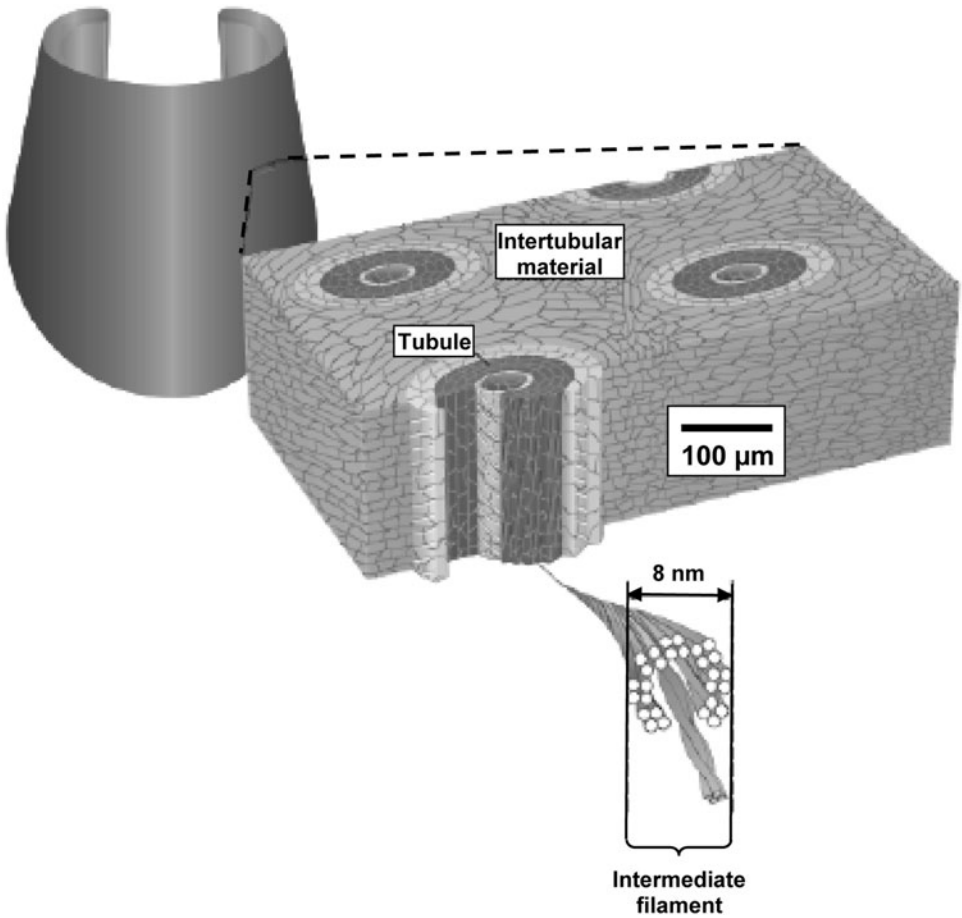

Fig. 13. Illustration of the front view of the equine hoof wall and a sketch of a hoof wall sample showing cells forming tubules and intertubular material. Intermediate filaments are drawn on the lamella of the cut-away tubule.[61] Adapted from Kasapi and Gosline [61].

The tongue of the hagfish (cartilaginous plate) has two rows of sharp teeth, as shown in Fig. 12a. The teeth are used to seize and hold prey. Human teeth have a thin layer of keratin (Nasmyth's membrane) on the enamel in the fetal stage, which is eventually worn away through mastication.

Hagfish Slime

Hagfish produce a mucus-like, viscous substance from their body when startled (Fig. 12b). This slime is composed of mucins and seawater, held together by long protein threads.[54] The slime reacts with water and clogs the gills of the predator fish, an effective and unique defense mechanism.[55] The slime is produced at an astonishing speed, and one hagfish can produce enough slime to clog a 20-L bucket of water in minutes. The slime contains threads that have an α-keratin-like IF structure.[56,57] The thread bundles are aligned, 1–3 μm in diameter, and are several centimeters long.[58,59] Because the threads are not encased in a matrix, useful studies have been performed to evaluate the bulk mechanical properties of pure keratin IFs.[5,57] Studies of these bundles are analogous to studies of tendons, which are aligned nonmineralized collagen fibrils. Figure 12c shows a comparison between tensile stress–strain curves for wet wool and hagfish threads. The initial slope of wool fibers is orders of magnitude higher than the hagfish threads; however, the maximum failure strain is four times lower. The initial Young's modulus of the hagfish slime is low—6 MPa—which is attributed to significant direct hydration of the IFs, which are normally shielded by the matrix in hard α keratins. The mechanical response of dry slime is significantly different from that of the wet one. The Young's modulus of the dry slime is 7.7 GPa, which is much higher than that of the wet slime and more similar to other keratin materials. This extreme dependence on the degree of hydration is a characteristic of most biological materials.

MOTION

Hooves

Similar to horns, hooves contain tubules $\sim$220 $\times$ 140 μm in major and minor axis, respectively, with a medullary cavity of $\sim$50 μm. These tubules are oriented in the longitudinal direction (parallel to the leg). The keratin forms in circular lamellae (5–15 μm thick) surrounding the tubules, as shown in Fig. 13.[9] It was concluded that the tubules serve only a mechanical function—to increase crack deflection, thereby increasing the toughness, making the equine hoof a highly fracture-resistant biological material.[9,60] The hooves must support large compressive and impact loads and must provide some shock absorption from the impact. The most thorough studies have been from Gosline and coworkers.[9,60–63] Bertram and Gosline[63] measured the effect of hydration on the tensile and fracture properties. They found the elastic modulus to decrease dramatically in the hydrated condition, ranging from 14.6 GPa (ambient) to 0.4 GPa (100% RH). Water penetrates the intertubular matrix as well as the amorphous polymer surrounding the keratin fibers, acting as a plasticizer, thereby decreasing the density and stiffness of the material.[37]

Fracture toughness was found maximum at 75% RH (22.8 kJ/m^2). Kasapi and Gosline[9,61] tested stiffness, tensile strength, and work of fracture in fully hydrated conditions to correlate the IF volume fraction and alignment with mechanical properties. They found the stiffness increased toward the outer hoof wall ranging from 0.30 GPa at the inner region to 0.56 GPa on the outer surface of the hoof wall, despite the porosity increase in that direction. The increase in elastic modulus was attributed to an increase in the volume fraction of IFs. Subsequent studies revealed the stiffness reinforcement was caused by the IFs volume fraction rather than the IF orientation. In the tubular material, the IFs are aligned in the tubule direction. However, they are aligned perpendicular to the tubule direction in the intertubular matrix. These different orientations help resist crack propagation through crack redirection, suggesting that the hoof wall structure evolved to maximize the fracture toughness.[61]

Bovine hooves are similar to equine hooves in both structure and properties,[7,64] as shown in Table II. Baillie and Fitford[65] described the bovine hoof structure as comprised of tubules embedded in intertubular material. Franck et al.[7] determined the tensile, compressive, and bending strengths and stiffness values. They are similar to the ones for equine hooves, considering the slightly different moisture content. Clark and Petrie[64] found the fracture toughness for bovine hooves (J-integral 8.5 kJ/m^2) to be lower than for the equine ones (J-integral 12.0 kJ/m^2).[62] Bendit and Kelly[14] found the elastic modulus to be dependent strongly on the relative humidity, which varied from 2 GPa (RH 65%) to 0.03 GPa (RH 100%).

The structural differences found between the bovine and equine hooves seem to mainly affect the toughness. The bovine tubule wall is thinner and the keratin cells in the intertubular material are more oriented parallel to the tubules than in the equine hoof. Accordingly, the intertubular IFs are more aligned in the direction of the tubules compared with those of equine hoof. Finally, in the bovine hoof, the interaction between tubular and intertubular material seems to be stronger than in the equine hoof, indicating a stronger interface. These differences account for the higher fracture toughness of the equine hoof compared with the bovine hoof.

Feathers

Feathers are the most complex integumentary appendages on all vertebrates.[66] They serve a variety of functions that includes flight, camouflage, courtship, thermal insulation, and water resistance. Feathers form from follicles in the epidermis that are periodically replaced by molting. The two main types of feathers are contour and down. The contour feathers cover the entire body with the insulating down feathers beneath them. Most studies on feathers have focused on two types of contour feathers—the remiges (wing) and the retrices (tail). Feathers are comprised of β keratin and melanin (which provides color).

The feather has a hierarchical construction based on a primary shaft, or rachis consisting of a cortex that encloses a cellular core, composed of uniformly sized cells of $\sim$20 μm in diameter. The rachis supports barbs, which are secondary keratinous features that form the herringbone pattern of the vane (Fig. 14).[67] Similarly, the barbs support tertiary features, including barbules.

The bulk of the cortex is constructed of fibers that measure 6 μm in diameter, which are aligned predominantly along the length of the shaft. These fibers are comprised of fibrils measuring 300–500 nm in diameter. The most superficial layer (cuticle) of the cortex is distinguishable from the bulk of the cortex in that it consists of circumferentially oriented fibers.[68,69] The feather can be described as a paradigm of a sandwich-structured composite,[70] and the cortex itself is a hierarchical, bilaminate, fiber-reinforced composite.

Some attempts to identify interspecies variations in Young's modulus of rachis keratin sampled from the dorsal surface of the cortex have been reported in the literature. Bonser and Purslow[71] tested cortex strips of the rachis on three outermost wing feathers sampled from eight species of birds. They reported that the interspecies variations in mechanical properties were low. The mean Young's modulus of the feather cortex was found to be 2.5 GPa, and with few exceptions, the interspecific differences were not statistically significant. The mass of the species studied represents a range of almost three orders of magnitude (0.06–10 kg); therefore, the authors reported that the stiffness of the cortex does not vary with mass of the bird. Previously, MacLeod[72] tested the segments of intact rachis (rachis segments in which the medullary core had not been separated from the cortex) from three species of landfowl and from a Herring Gull. In

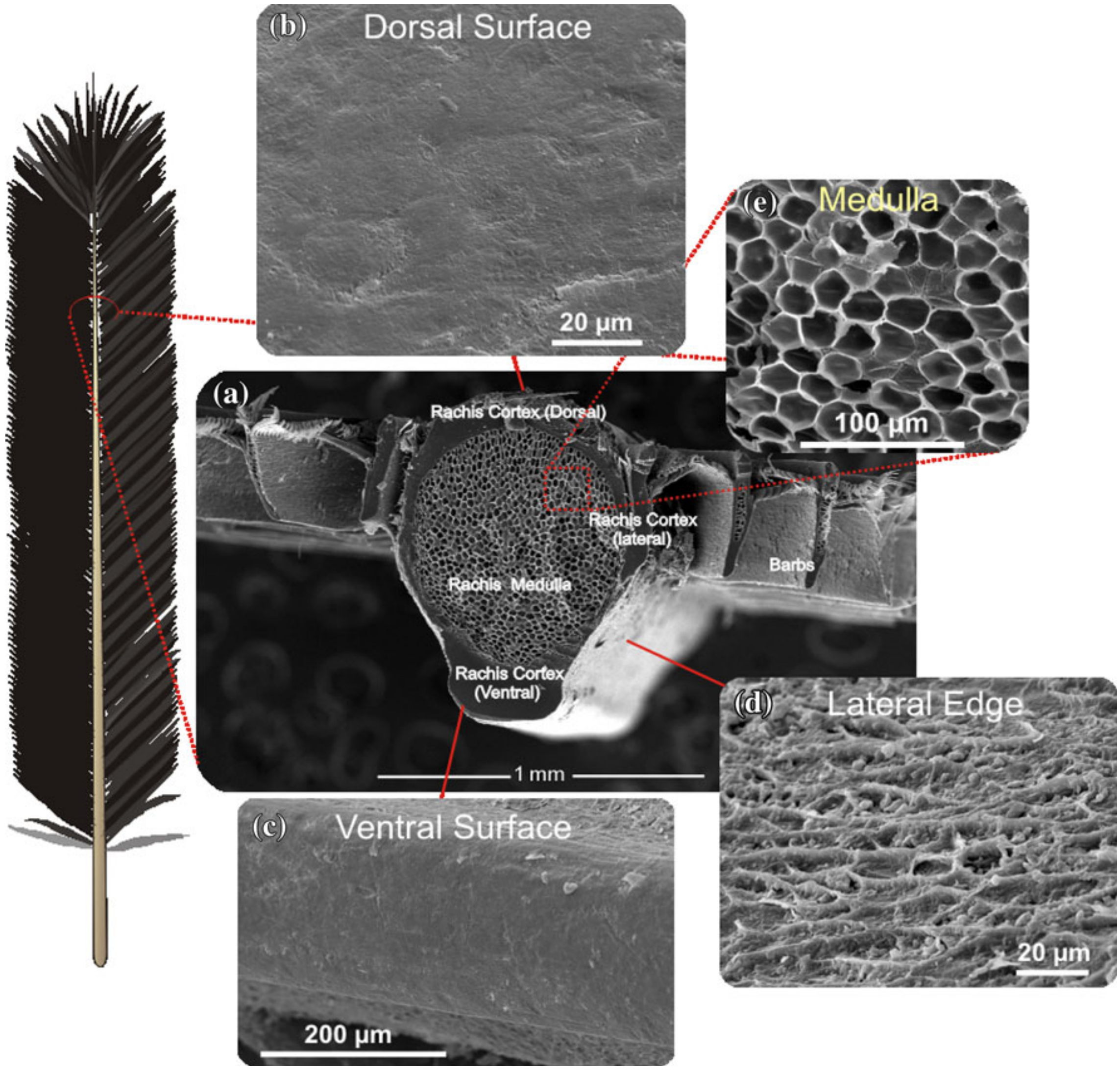

Fig. 14. SEM of the surface microstructure of the cortex and (a) the cross section of a distal section of rachis. The (b) dorsal and (c) ventral cortical rachis is smooth at the microscale, whereas the (d) lateral cortical rachis keratin is fibrous and textured with ridges separated by 10–20 μm. The cortex encloses (e) a medullary core constructed of cells ranging from 20 μm to 30 μm in diameter[67]

contrast to the conclusion reported by Bonser and Purslow,[71] for both tension and flexure, the interspecies variation in Young's modulus was high; for cortex from which the medulla had been removed, the tensile Young's modulus ranged from 1 MPa to 8 MPa, where uncertainty was reported as $\sim$10%.[72] The discrepancy in the literature may be a result of differences in the sampling technique, treatment, and environmental conditions (e.g., the mechanical performance of feather is reported to be humidity sensitive[4,73]), although interspecific microstructural variation may play a role.

Significant differences were identified as a function of position along the length of the rachis.[71,74] The distal (furthest from body) region of the feather is more mature than the proximal region (closest to body), and morphology is substantially different along the length,[75] in terms of size, cross-sectional geometry, and thickness of the cuticle.[68,69] This was reported in cortical rachis along a single wing feather of a Mute Swan, which is one of the most massive of the flying species of birds.[71] The Young's modulus from the proximal end to the distal tip, based on tension testing of dorsal (top surface of feather rachis) cortex strips, was found to increase linearly, from 1.8 GPa to 3.8 GPa.[71] This trend was reported to be absent in the rachis of the flightless ostrich.[76] Bostandzhiyan et al.[74] reported failure strengths of dorsal section of cortex collected from a goose to be 188–240 MPa at the calamus and 74 MPa at a more distal section, whereas Weiss and Kirchner[77] reported an inverse trend for the tail coverts of a wild-type peacock, a generally cursorial (running) species. Therefore, for birds capable of flight, temporal effects and fiber alignment gradients from the proximal to distal end may contribute

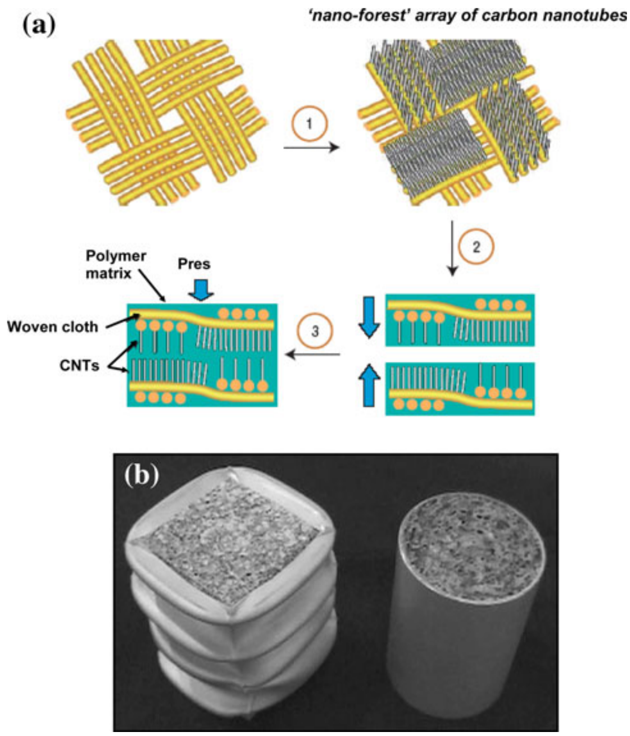

Fig. 15. (a) Aluminum shell filled with aluminum foam for automotive applications. Right: initial configuration. Left: compressed along longitudinal axis showing plastic buckling.[38] (b) Using a carbon nanotube forest, the laminates in this composite are stitched together to form a stronger, stiffer composite[81]

to an increase of at least 100% in stiffness or a decrease in failure strength by more than 200%. Bodde et al.[67] investigated the tensile properties of the tail feathers of the Toco Toucan. The dorsal and ventral surfaces of the cortex are both significantly stiffer and stronger than the lateral surface. The distal end of the feather was found to be more stiff and weaker than those sampled from the proximal and middle regions. Distinctive fracture patterns correspond to the failure in the superficial cuticle layer and the bulk of the rachis cortex. In the cuticle, where supramolecular keratinous fibers are oriented tangentially, evidence of ductile tearing was observed. In the bulk cortex, where the fibers are bundled and oriented longitudinally, patterns suggestive of near-periodic aggregation and brittle failure were observed.

BIOINSPIRED STRUCTURES

The study of structural biological materials shed insights into how are organisms assemble tough, lightweight structures. The design concept of the porcupine quill has synthetic structure parallels in many fields, such as in aviation, offshore oil platforms, and scaffolds in the medical field.[78–80] Karam and Gibson[34] suggested the structure of the hedgehog spine is optimally designed to resist buckling loads. Figure 15a shows an aluminum tube filled with aluminum foam and subjected to compressive loading beyond the onset of plastic instability. The characteristic buckling pattern is analogous to that of the quill subjected to the same loading (Fig. 7). Thus, the mechanisms of reinforcement are similar.

The sheep horn has keratin filaments that are not only embedded parallel to the growth direction but also extend from one layer to the next. These cross-ply fibers aid in decreasing delamination by holding the layers together strongly. Composite materials companies recognize that delamination is the most common failure mode for layered composite materials and have fabricated composites that are cross stitched together. However, although this process improves the delamination strength, the presence of the holes from stitching decreases the overall fracture strength. A novel composite that is similar to the structure of animal horns is shown in Fig. 15b.[81] A "forest" of carbon nanotubes is grown on the surface of the laminate, which then holds the plies together. This resulted in enhanced mechanical properties. The fracture toughness was increased by $\sim$350%, the flexural modulus increased by $\sim$100%, and the flexural toughness increased by $\sim$525% over the base composite.

Hagfish slime threads have received recent interest from the biotechnology field. They make a good candidate for high-performance fiber threads that could build materials that rival synthetic ones (Kevlar [Dupont Advanced Fibers Systems, Richmond, VA], nylon, and polyester) for ballistics protection.

CONCLUSIONS

Keratin is a lightweight (1.3 g/cm^3) robust structural biological material that serves a variety of functions, from simple waterproofing to impact-resistant structures (hooves and horns). It has excellent mechanical properties in both tension and compression. The scaly or tiled appearance of the surface is that most keratin is produced in cells, which die after full keratinization, leaving the cell wall remnants around the keratinized material. Hard keratin (α and β) is a composite material composed of short crystalline fibers (IFs) embedded in a highly cross linked elastomeric matrix. This matrix can be compared with vulcanized rubber.

Keratinaceous materials have four major morphologies:

1. Dense waterproof layer (osteoderms and skin)
2. Dense shells filled with a porous material, resulting in the formation of lightweight, stiff, buckle-resistant structures (quills, feathers, and bird beaks)
3. Solid blocks with embedded tubules that are impact resistant (hooves and horns)
4. Filamentary forms (gecko feet and hagfish slime)

It is well known that good bonding is needed between the fiber and the matrix in a polymer composite, which is accomplished well in keratin, through chemical bonding by sulfur cross links between the fiber and the matrix. The mechanical properties of keratin, like most biological materials, are extremely sensitive to the amount of hydration, with stiffness and strength decreasing accompanied by an increase in toughness with increasing hydration. The volume fraction and orientation of the IFs also influence the mechanical properties.

ACKNOWLEDGEMENTS

We thank James Kiang for help with the feathers and Christy Chao for help with the quills. This work is supported by Research Grant 1006931 from the National Science Foundation, Division of Materials and Grant 100-2218-E-007-016-MY3 from the Taiwan National Science Council.

REFERENCES

1. M. Feughelman, *Textile Res. J.* 29, 223 (1959).
2. S.A. Wainwright, W.D. Biggs, J.D. Currey, and J.M. Gosline, *Mechanical Design in Organisms* (Princeton, NJ: Princeton University Press, 1982).
3. Y. Seki and M.A. Meyers, *Acta Mater.* 53, 5281 (2005).
4. A.M. Taylor, R.H.C. Bonser, and J.W. Farrent, *J. Mater. Sci.* 39, 939 (2004).
5. D.S. Fudge and J.M. Gosline, *Proc. R. Soc. Lond. B* 271, 291 (2004).
6. H.P. Baden and P.F. Maderson, *J. Exp. Zool.* 174, 225 (1970).
7. A. Franck, G. Cocquyt, P. Simoens, and N. De Belie, *Biosyst. Eng.* 93, 459 (2006).
8. I.P. Wagner, D.M. Hood, and H.A. Hogan, *Am. J. Vet. Res.* 62, 745 (2001).
9. M.A. Kasapi and J.M. Gosline, *J. Exp. Biol.* 200, 1639 (1997).
10. A. Kitchener, *J. Mater. Sci. Lett.* 6, 321 (1987).
11. F.L. Warburton, *J. Textile Inst.* 39, 297 (1948).
12. L. Tombolato, E.E. Novitskaya, P.-Y. Chen, F.A. Sheppard, and J. McKittrick, *Acta Biomater.* 6, 319 (2010).
13. L. Farran, A.R. Ennos, M. Starkie, and S.J. Eichhorn, *J. Biomech.* 42, 1230 (2009).
14. E.G. Bendit and M. Kelly, *Textile Res. J.* 48, 674 (1978).
15. W. Yang, C. Chao, E.E. Novitskaya, and J. McKittrick (unpublished work, University of California San Diego, La Jolla, CA, 2011).
16. S.F. Chou and R.A. Overfelt, *Mater. Sci. Eng. C* 31, 1729 (2011).
17. J.F.V. Vincent and P. Owers, *J. Zool.* 210, 55 (1986).
18. Y. Papir, K. Hsu, and R. Wildnauer, *Biochim. Biophys. Acta* 399, 170 (1975).
19. R. Meredith, ed., *The Mechanical Properties of Textile Fibers* (Amsterdam, The Netherlands: North Holland Publishing Co., 1956).
20. R.D.B. Fraser and T.P. MacRae, *The Mechanical Properties of Biological Materials, Symposium of the Society of Experimental Biology,* ed. J.F.V. Vincent and J.D. Currey (Cambridge, UK: Cambridge University Press, 1980), pp. 211–246.
21. D.A.D. Parry and A.C.T. North, *J. Struct. Biol.* 122, 67 (1998).
22. D. Voet, J.G. Voet, and C.W. Pratt, *Biochemistry: Life at the Molecular Level*, 3rd ed. (New York, NY: John Wiley & Sons, 2008).
23. B.M. Chapman, *J. Textile Inst.* 60, 181 (1969).
24. J. McKittrick, P.-Y. Chen, L. Tombolato, E.E. Novitskaya, W. Trim, Y.-S. Lin, G.A. Hirata, E.A. Olevsky, M.F. Horstemeyer, and M.A. Meyers, *Mater. Sci. Eng. C* 30, 331 (2010).
25. H. Yamada, *Strength of Biological Materials* (Baltimore, MD: F.G. Williams and Wilkins, 1970).
26. H. Zahn, J. Föhles, M. Nienhaus, A. Schwan, and M. Spei, *Ind. Eng. Chem. Proc. Res. Dev.* 19, 496 (1980).
27. R.D.B. Fraser, T.P. MacRae, D.A.D. Parry, and E. Suzuki, *Polymer* 12, 35 (1969).
28. A. Park and C. Baddiel, *J. Soc. Cosmet. Chem.* 23, 3 (1972).
29. R.D. Fraser, T.P. MacRae, D.A. Parry, and E. Suzuki, *Proc. Natl Acad. Sci. USA* 83, 1179 (1986).
30. J.W.S. Hearle, *Int. J. Biol. Macromol.* 27, 123 (2000).
31. F.J. Wortmann and H. Zahn, *Textile Res. J.* 64, 737 (1994).
32. M. Feughelman, *Mechanical Properties and Structure of α-Keratin Fibres: Wool, Human Hair and Related Fibres* (Sydney, Australia: University of New South Wales Press, 1997).
33. L. Peters and H.J. Woods, *The Mechanical Properties of Textile Fibers,* ed. R. Meredith (Amsterdam, The Netherlands: North Holland Publishing Company, 1955), pp. 151–163.
34. G.N. Karam and L.J. Gibson, *Mater. Sci. Eng. C* 2, 113 (1994).
35. L.J. Gibson and M.F. Ashby, *Cellular Solids: Structure and Properties* (New York, NY: Pergamon Press, 1988).
36. L.J. Gibson, M.F. Ashby, G.N. Karam, U. Wegst, and H.R. Shercliff, *Proc. R. Soc. Lond. A* 450, 141 (1995).
37. J.F.V. Vincent, *Structural Biomaterials*, Revised ed. (Princeton, NY: Princeton University Press, 1990).
38. J. Banhart, *MRS Bull.* 28, 290 (2003).
39. A. Kitchener, *J. Zool.* 213, 621 (1987).
40. A. Kitchener and J.F.V. Vincent, *J. Mater. Sci.* 22, 1385 (1987).
41. A. Kitchener, *J. Zool.* 214, 1 (1988).
42. A.C. Kitchener, *Biomechanics and Evolution*, ed. J.M.V. Rayner and R.J. Wootton (Cambridge, UK: Cambridge University Press, 1991).
43. A.C. Kitchener, *Biomechanics in Animal Behaviour*, ed. P. Domenici and R.W. Blake (Oxford, UK: BIOS Scientific Publishers, 2000).
44. W. Trim, M.F. Horstemeyer, H. Rhee, S.-J. Park, H. El Kadiri, L. Williams, J. Liao, and J. McKittrick, *Acta Biomater.* 7, 1228 (2011).
45. S. Lee, B. Reyante, T. Tsukasa, E. Wooley, L. Tombolato, P.-Y. Chen, E.E. Novitskaya, J. Vasquez, R. Urbaniak, and J. McKittrick, *Mater. Sci. Eng. C* 31, 730 (2011).
46. R.H.C. Bonser, *J. Mater. Sci. Lett.* 19, 1039 (2000).
47. R.H.C. Bonser, *J. Mater. Sci. Lett.* 21, 1563 (2002).
48. L. Farran, S. Shayler, and A.R. Ennos, *J. Exp. Biol.* 207, 735 (2004).
49. L. Farran, A.R. Ennos, and S.J. Eichhorn, *J. Exp. Biol.* 211, 3677 (2008).
50. Y. Seki, B. Kad, D. Benson, and M.A. Meyers, *Mater. Sci. Eng. C* 26, 1412 (2006).
51. Y. Seki, S.G. Bodde, and M.A. Meyers, *Acta Biomater.* 6, 331 (2010).
52. G.N. Karam and L.J. Gibson, *Int. J. Solids Struct.* 32, 1259 (1995).
53. M.M. Smith and M.L. Coates, *Development, Function and Evolution of Teeth*, ed. M.F. Teaford, M.M. Smith, and M.W.J. Ferguson (Cambridge, UK: Cambridge University Press, 2007), p. 137.
54. D.S. Fudge, N. Levy, S. Chiu, and J.M. Gosline, *J. Exp. Biol.* 208, 4613 (2005).
55. J. Lim, D.S. Fudge, N. Levy, and J.M. Gosline, *J. Exp. Biol.* 209, 702 (2006).
56. S.W. Downing, R.H. Spitzer, E.A. Koch, and W.L. Salo, *J. Cell Biol.* 98, 653 (1984).
57. D.S. Fudge, K.H. Gardner, V.T. Forsyth, C. Riekel, and J.M. Gosline, *Biophys. J.* 85, 2015 (2003).
58. S. Downing, R.H. Spitzer, W.L. Salo, S.D. Downing, L.J. Saidel, and E.A. Koch, *Science* 212, 326 (1981).
59. B. Fernholm, *Acta Zool.* 62, 137 (1981).
60. M.A. Kasapi and J.M. Gosline, *Equine Vet. J.* 26, 10 (1998).
61. M.A. Kasapi and J.M. Gosline, *J. Exp. Biol.* 202, 377 (1999).

62. J.E.A. Bertram and J.M. Gosline, *J. Exp. Biol.* 125, 29 (1986).
63. J.E.A. Bertram and J.M. Gosline, *J. Exp. Biol.* 130, 121 (1987).
64. C. Clark and L. Petrie, *Vet. J.* 173, 541 (2007).
65. C. Baillie and R. Fitford, *Biomimetics* 4, 1 (1996).
66. A.M. Lucas and P.R. Stettenheim, *Agricultural Handbook*, Vol. 362 (Washington, DC: Government Printing Office, 1972).
67. S.G. Bodde, M.A. Meyers, and J. McKittrick, *J. Mech. Behav. Biomed. Mater.* 4, 723 (2011).
68. C. Earland, P.R. Blakey, and J.G.P. Stell, *Nature* 196, 1287 (1962).
69. C. Earland, P.R. Blakey, and J.G.P. Stell, *Biochim. Biophys. Acta* 56, 268 (1962).
70. D.G. Crenshaw, *Symp. Soc. Exp. Biol.* 34, 485 (1980).
71. R.H.C. Bonser and P.P. Purslow, *J. Exp. Biol.* 198, 1029 (1995).
72. G.D. MacLeod, *J. Exp. Biol.* 87, 65 (1980).
73. R.H.C. Bonser and J.W. Farrent, *Br. Poult. Sci.* 42, 271 (2001).
74. S.A. Bostandzhiyan, A.S. Shteinberg, and A.V. Bokov, *Dokl. Akad. Nauk SSSR* 408, 772 (2006).
75. P.O. Prum, *J. Exp. Zool.* 285, 291 (1999).
76. G. Cameron, T. Wess, and R. Bonser, *J. Struct. Biol.* 143, 118 (2003).
77. I.M. Weiss and H.O.K. Kirchner, *J. Exp. Zool.* 313A, 690 (2010).
78. V. Karageorgiou and D. Kaplan, *Biomaterials* 26, 5474 (2005).
79. A. Cao, V.P. Veedu, X. Li, Z. Yao, M.N. Ghasemi-Nejhad, and P.M. Ajayan, *Nat. Mater.* 4, 540 (2005).
80. M.A. Lopez-Heredia, J. Sohier, C. Gaillard, S. Quillard, M. Dorget, and P. Layrolle, *Biomaterials* 29, 2608 (2008).
81. V.P. Veedu, A. Cao, X. Li, K. Ma, C. Soldano, S. Kar, P.M. Ajayan, and M.N. Ghasemi-Nejhad, *Nat. Mater.* 5, 457 (2006).